UNIVERSITY OF CALIFORNIA

SANTA CRUZ

IN VIVO MEASUREMENTS OF LUNG VOLUMES IN RINGED SEALS: INSIGHTS FROM BIOMEDICAL IMAGING

This thesis has been approved in partial satisfaction
of the requirements for the degree of

MASTER OF SCIENCE

in

OCEAN SCIENCES

by

HOLLY HERMANN-SORENSEN

September 2020

The Thesis of Holly Hermann-Sorensen
is approved:

____
Dr. Colleen Reichmuth, Chair

____
Dr. Terrie M. Williams

____
Dr. Andrew Moore

____
Quentin Williams
Interim Vice Provost and Dean of Graduate Studies

Table of Contents

Acknowledgements iv

Abstract viii

Introduction 1

Methods 3

- Subjects & Animal Handling 3
- Volumetry 6
- Allometry 7
- Body density and buoyant force 8

Results 8

- Volumetry 8
- Allometry 10
- Body density and net buoyant force 10

Discussion 11

References 16

Tables & Figures 22

Appendices 26

Acknowledgements

I would like to express my deepest gratitude to my advisor, Dr. Colleen Reichmuth for her unwavering belief in, and encouragement of the graduate students that come through her lab. The lab's custom of operating in an "all for one, one for all" manner is ingrained in everyone who walks through the compound doors, and is what has shaped me as a leader, animal trainer, and scientist in the lab. My best memories of graduate school were made traveling to Alaska with Colleen, in the long nights spent preparing data and marveling over how incredibly lucky we are to study ice seals. These quiet, inquisitive, Earl Grey tea and Biscoff/Saltine cracker-fueled evenings are something I will truly miss. I'll never forget her mantra to "work the problem", or to put others before me as she invariably does for the lab, its animals, and its people.

I am incredibly thankful to Dr. Nicole Thometz, an incredible mentor, scientist, and one of my greatest inspirations. Nicole taught me everything I know about physiology and has opened countless doors for me on my journey through graduate school. I am eternally grateful for her confidence in me to work on the PHOCAS project, and I hope that I may one day asymptotically reach her level of poise and professionalism.

To Dr. David Rosen, I am thankful for his insight into my project, whatever it may have been at the time. Dave is the epitome of the brilliant scientist who is so good at what they do, they can get away with almost anything (including rapping about his research at a major conference).

Dr. Kathy Woodie is an extraordinary veterinarian, from whom I've learned a great deal during my time in Alaska. Her willingness to teach and lead by example is admirable, and I'm forever grateful for the experiences I've had working alongside her and the Arctic seals.

Dr. Sophie Dennison-Gibby is an exceptional veterinary radiologist; I greatly appreciate the time she spent assisting me with identifying specific anatomical structures within CT scans, and for encouraging me to publish this work.

My fellow lab mates at the Pinniped Lab have been a resolute support system throughout my time in the program. Jenna Lofstrom, whose job title encompasses so much more than Lab Manager—I will miss her more than she knows. She flawlessly steers the lab's ship through narrow channels and keep us laughing along the way. I will severely miss our time together but have so many amazing and hilarious memories to hold onto.

My close friend and forever lab mate Michelle Hartwick is a beacon of light on my darkest days and a true soul (seal) sister. I am proud to have a friend like her; she continues to inspire me to be tenacious in my endeavors by doing so herself.

I would like to acknowledge Dr. Jeppe Have Rasmussen for his selfless help during the beginning stages of this project. Jeppe mentored and assisted me in developing a MATLAB script to analyze the CT data, and while I pivoted to using a different software, I am incredibly grateful for his assistance and positive attitude during script troubleshooting.

I am indebted to Dr. Paul Martre, a man whom I've never met in person, yet became a friend and mentor to me online. His YouTube channel and software expertise launched me like a pinball into the world of 3D reconstructions of CT scans. I can say without a doubt that without the patience, kindness, and help of this incredible stranger, I would be lost.

I am incredibly grateful to my committee members, Dr. Terrie Williams and Dr. Andrew Moore, who patiently awaited my thesis and provided thoughtful feedback and encouragement. Their positivity and support leading up to receiving my thesis was refreshing, and I thank them for their commitment to my success.

My partner, Nick, has been my ardent supporter, encouraging me and loving me unconditionally through it all. I cannot imagine going through my life without him by my side (or 2,000 miles away, as it sometimes were). Nick provided me constant reminders of my wins when it sometimes felt like a slew of setbacks and forced me into nature when my work-life balance was all the former. I always returned from these excursions feeling renewed and more centered, and for that I am extremely blessed to have someone like him in my life.

Finally, but certainly not least of all, to my Alaska team both human and animal alike—thank you for welcoming me with open arms (and flippers) to Seward during

my first summer spent in Alaska. It was here that I forged friendships among the hardest-won, most determined and courageous people I've ever met. Alaskans have an immense amount of grit that I only aspire to possess in my life on the other side of academia. My time spent working with the Arctic seals is something I'll cherish forever; the environment both physically and mentally only permits the hardiest individuals to reside in this vast and wild state, and I look forward to returning to rekindle the untamed spirit that makes me feel beholden to this place.

Abstract

***IN VIVO* MEASUREMENTS OF LUNG VOLUMES IN RINGED SEALS: INSIGHTS FROM BIOMEDICAL IMAGING**

Holly Hermann-Sorensen

Marine mammals rely on oxygen stored in blood, muscle, and lungs to support breath-hold diving and foraging at sea. Here, we used biomedical imaging to examine lung oxygen stores and other key respiratory parameters in living ringed seals (*Pusa hispida*). Three-dimensional models created from CT images were used to quantify total lung capacity (TLC), respiratory dead space, minimum air volume, and total body volume to improve assessments of lung oxygen storage capacity, scaling relationships, and buoyant force estimates. Results suggest that lung oxygen stores determined *in vivo* are smaller than those derived from typical postmortem measurements. We also demonstrate that—while established allometric relationships hold well for most pinnipeds—these relationships consistently overestimate TLC for the smallest phocid seal. Finally, measures of total body volume reveal differences in calculated body density and net buoyant force that would influence costs associated with diving and foraging in free-ranging seals.

Introduction

A key question in marine mammal physiology is how air-breathing vertebrates remain active under water for long periods on a single breath (Butler and Jones, 1997; Ponganis, 2015; Scholander, 1940). To support diving, marine mammals rely on oxygen reservoirs compartmentalized in blood, muscle, and lungs. The blood and muscle oxygen stores are well-studied in marine mammals relative to the lungs. This can be attributed to a reduced dependence on pulmonary oxygen stores in marine mammals relative to terrestrial species, as well as the difficulty of obtaining quantitative measurements from living, freely-diving individuals (Ponganis and Williams, 2016).

Key metrics for evaluating respiratory function include minimum air volume (MAV) and total lung capacity (TLC). MAV is the minimum volume of air in relaxed lungs (Fahlman et al., 2011; Kooyman, 1973), while total lung capacity refers to lung volume at maximum inhalation or when manually inflated to a standard air pressure of 30 cm H_2O or 22 mmHg (Denison et al., 1971). TLC is not easily determined in living animals; for this reason, a variety of techniques are often employed to determine other respiratory parameters, which are then used to estimate TLC (Wanger et al., 2005). These methods include nitrogen washout (Sue, 2013), whole body plethysmography (Kooyman et al., 1972; Lenfant et al., 1970), and various respirometry approaches (Scholander, 1940). In addition, allometric scaling relationships derived from empirical measurements provide a means to estimate TLC from body mass when species data are not available. For marine mammals, the most commonly utilized relationships are usually adopted from Kooyman (1973, 1989). However, these scaling relationships have not been updated recently, and source data for TLC often include pooled values of mixed age classes. Even so, these relationships have been used ubiquitously with the assumption that they hold across a wide range of body sizes and age classes.

TLC and MAV can be measured postmortem (Burns et al., 2007; Denison et al., 1971; Fahlman et al., 2011; Kooyman and Sinnett, 1979; Lydersen et al., 1992; Mitchell and Skinner, 2011) by excising the complete respiratory tract and measuring associated water displacement in both non-inflated (resting) conditions (i.e. MAV) and inflated conditions (i.e. TLC). The difference in displacement in each condition is related to the volume of the respiratory tract. Researchers interested in mammalian diving physiology rely on these postmortem estimates despite there being little information regarding the reproducibility of *ex situ* values in living animals (Fahlman et al., 2020), with only a handful of studies directed at comparing pulmonary function and positioning both *in situ* and *ex situ* in individuals (Chevalier et al., 1978; Fahlman et al., 2014; Soutiere and Mitzner, 2004; Standaert et al., 1985).

Biomedical imaging has emerged as a valuable tool to examine respiratory anatomy in animals (Moore et al., 2011; Ponganis et al., 1992; Smodlaka et al., 2009), including the air reservoirs within living animals such as mice (Mitzner et al., 2001), dogs (Chevalier et al., 1978), and seabirds (Nevitt et al., 2014; Ponganis et al., 2015). In these cases, air spaces can be visualized and quantified using three-dimensional reconstructions of respiratory structures in both postmortem and living, anesthetized individuals. Importantly, this approach also allows for the calculation of a subject's body volume (Ponganis et al., 2015), which can be used to determine body density and buoyant forces while diving.

In this study, we opportunistically used computed tomography (CT) imaging data obtained during routine veterinary procedures to examine *in vivo* lung volumes, capacities, and whole-body buoyant force in living ringed seals (*Pusa hispida*). Small body size and ease of handling enabled high-resolution volumetric quantification of discrete respiratory structures, including the anatomical dead space and individual lungs, as well as whole-body volume. We report key respiratory variables in the smallest phocid species, provide insight into the applicability of commonly used allometric scaling relationships, and discuss the ecological implications of this work for free-ranging ringed seals.

Methods

Subjects & Animal Handling

One female and three male ringed seals (1.3-3.6 y) were evaluated. Age was estimated from the length, weight, and overall development of each individual at intake to rehabilitative care at the Alaska SeaLife Center (Seward, Alaska USA). Length and mass were determined within one week of the CT procedure. Standard length (linear distance from nose through tail) was either directly measured on the day of the CT procedure or measured from full body scans. Animal mass was obtained via platform scale (W.C. Redmon Co., Peru, IN USA or Ohaus SD751, Ohaus Corp., Parsippany, NJ USA). Two individuals (PH1701 and PH1804) presented with verminous pneumonia at intake and were treated with anti-helminthic drugs during rehabilitation, with resolution prior to imaging. Thus, the scans included in this study represent healthy individuals cleared of parasites, with no pathological evidence for lungworm infection present at the time of the scans.

Seals were briefly restrained at the Alaska SeaLife Center and given a pre-anesthetic intramuscular injection of Midazolam (0.2-0.5 mg kg^{-1}) and Butorphanol (0.24-0.7 in mg kg^{-1}) (see Woodie et al., 2020). Following sedation, a single lumen central venous catheter (16-18 g, 13-15 cm) was placed in the epidural vertebral sinus flushed with heparinized saline and capped as in Goertz et al. (2008). Patency of the soft catheter was ensured prior to transport to the nearby imaging facility. Prior to the CT procedure, Propofol (2-3 mg kg^{-1}) was administered intravenously via the catheter and titrated incrementally to facilitate apneic intervals during scanning with manual, intermittent, positive-pressure ventilation prior to and following each imaging series. Following intubation and inflation of an endotracheal tube cuff, seals were maintained on oxygen and isoflurane gas for the duration of the procedure. Full inflation of the cuff prevented air leakage around the tube. A nonsteroidal anti-inflammatory medication (Meloxicam, 0.2-0.5 mg kg^{-1}), and broad-spectrum antibiotic (Cefazolin, 10-20 mg kg^{-1}) were administered intravenously via the catheter. Following the CT procedure, sedation was reversed with separate injections of intramuscular or intravenous Naltrexone (2 mg Naltrexone per 1 mg Butorphanol) and intravenous Flumazenil (1 mg Flumazenil per 20 mg Midazolam). The endotracheal tube was removed after regular spontaneous respirations resumed. Following extubation, seals were returned to the Alaska SeaLife Center where they resumed normal eating and activity within an hour. Duration of anesthesia was less than one hour from Propofol induction to recovery and extubation.

CT scans were performed with a GE 16 Light Speed Scanner, GE 16 Bright Speed Scanner (General Electric Healthcare, Chalfont St. Giles, Bucks, UK), or a Siemens 32/64 Somatom GO-UP Scanner (Siemens, Munich, Germany). Modified chest protocols (Table S1; Dennison-Gibby, personal communication) were used to obtain high-resolution serial images of the full respiratory tract with slice thickness of 0.625 - 2.5 mm. An initial scan was obtained on two seals (PH1802 and PH1804) in ventral recumbency without lung inflation during apnea, with the pressure gauge of the anesthesia circuit at 0 mmHg. This condition was defined as the resting, relaxed position of the lungs. All seals were scanned in ventral recumbency with lungs hyperinflated to a pressure of 30 mmHg. To test for replicability of lung volume at a given pressure, variation in volume within inflation conditions, and the difference in volume as a result of patient position, one seal (PH1802) received additional scans in both dorsal and ventral recumbency at inflation pressures of both 30- and 37-mmHg.

Animal handling activities including rescue, rehabilitation and diagnostic CT procedures were authorized under NOAA's Marine Mammal Health and Stranding Response/Research Program 18786 and Stranding Agreement SA-AKR-2019-01.

Research was approved by the Institutional Animal Care and Use Committee at the University of California Santa Cruz.

Volumetry

To determine key respiratory parameters at known lung inflation conditions, DICOM images from CT series were imported to 3D Slicer (Fedorov et al., 2012, www.slicer.org) and converted into closed-surface three-dimensional models. Anatomical structures were manually separated into volumetric segmentations of trachea, bronchi, and left and right lungs based on tissue radiodensity (Figure 1). Tracheal volume was defined as the region immediately caudal to the laryngeal cartilages extending to the region just cranial to start of the carina. Bronchial volume was defined as the region from the carina to distal portions of the cranial and caudal lobar bronchi. Bronchioles were too diffuse to manually trace, so their volume is included in the volume of the lungs. Total lung volume included both the tissue and air spaces of the left and right lungs, in addition to the bronchioles. The inclusion of the tissue and air spaces are in line with other studies (Lydersen et al., 1992) to whom we compared our values. The volume of each segment was calculated in cubic centimeters and converted to milliliters.

Segments of the respiratory tract were considered with respect to whether surfaces were available for oxygen exchange. Anatomical dead space (the portion not in contact with gas exchange surfaces) was defined as the volume of the trachea plus the volume of the bronchi; this measure is not equivalent to respiratory dead space

(Fowler, 1948; Rossier and Bühlmann, 1955) as the bronchioles could not be partitioned from the tissues of the lungs in this study. MAV was characterized here as the lung volume in the non-inflated (resting) condition, with inflation pressure of 0 mmHg. TLC was determined as the volume of the inflated lungs at 30 mmHg; this inflation pressure is higher than the standard of 22 mmHg (30 cm H_2O) used to measure TLC in other mammalian studies (Denison and Kooyman, 1973; Denison et al., 1971; Kooyman and Sinnett, 1982; Loring et al., 2016; Moore et al., 2011; Weibel, 1973), but was necessary for the clinical protocol. To obtain the proportion of blubber that comprised the total body volume, blubber was segmented and quantified for the two animals in which we had whole body scans (PH1802 and PH1804). Further, surface area to volume ratio (SA:V) was directly measured for seal PH1802.

Allometry

To compare our results to those of other marine mammals, we considered the commonly used allometric scaling equation: $TLC=0.1M_b^{0.96}$ (Kooyman, 1989). We also determined another scaling equation specific to pinnipeds. The TLC data included in the pinniped-only allometric plot were either collected empirically or could be back-calculated from empirically reported mass-specific total lung oxygen stores. We evaluated our primary measure of mean total lung capacity (TLC) as a function of mean total body mass for the subadult ringed seals in our study. We then compared our results to expected values from these allometric relationships to determine whether total body mass is a reliable indicator of total lung capacity for ringed seals.

Body density and buoyant force

CT data were further used to estimate the whole-body buoyant force of two seals (PH1802 and PH1804) at specific lung inflation pressures, as in Ponganis et al. (2015). Body density was calculated by dividing body mass by total body volume and comparing to the density of seawater. Total body volume (mL) was determined by segmentation of the CT data as described above. Whole-body buoyant force was calculated for each seal at each lung inflation pressure, as follows (Eq.1):

$$\text{Eq. 1} \qquad \text{Buoyant force (N)} = [(g \times M_b \times \left[(\rho_{seawater}/\rho_{total\ body}) - 1\right]$$

where g is the acceleration of gravity at 9.807 (m s^{-2}), M_b is body mass in kilograms, $\rho_{seawater}$ is the density of seawater at 10ºC in g mL^{-1}, and $\rho_{total\ body}$ is the calculated density of the seal's body in grams per milliliter. Buoyant force was only calculated in the inflated condition for seal PH1804, as there was no full body scan available in the non-inflated condition. Buoyant force was calculated in both inflated and non-inflated conditions for seal PH1802, and total body volume was compared at the level of the whole animal relative to changes in the respiratory tract volume.

Results

Volumetry

Due to the clinical purpose of the scans, primary comparisons of respiratory structures and volumetric analyses were made at lung inflation pressures of 0- and 30-mmHg in ventral recumbency (Table 1). When inflated to a pressure of 30 mmHg, total lung volumes ranged from 870 to 2271 mL; resulting in mass-specific TLC values between 52 and 92 mL kg^{-1}. The right lung was larger than the left in all individuals in the inflated condition, with an average size difference of 6.3%. For two individuals measured in the non-inflated condition total lung volumes were 564 and 886 mL, with mass-specific MAV of 22 and 32 mL kg^{-1}. Lung volumes for these individuals increased by a factor of 2.5 when fully inflated.

The maximum total respiratory tract volume observed across all individuals was 904 to 2323 mL. This was equivalent to 11% and 18% of total body volume for the two seals with full body scans (PH1804 and PH1802). The anatomical dead portion of the respiratory tract changed little with inflation for two individuals with comparable non-inflated and inflated scans (PH1503 and PH1802). These seals exhibited similar increases in tracheal volume (~15%) and negligible increases in bronchi volume (~1%) from non-inflated to inflated conditions. Thus, while the volume of the total respiratory tract changed by an average factor of 2.5 when the lungs were inflated, most of this difference was due to changes in lung volume.

Replicate scans in ventral recumbency at 37 mmHg for seal PH1802 showed that lung volume varied by 5% (74 mL) between scans. Lung volume varied similarly between 30- and 37-mmHg, with an increase of 5% (75 mL) at the higher inflation pressure. Total lung volume was 13% (194 mL) greater in dorsal recumbency than in ventral recumbency at the same inflation pressure (37 mmHg).

Full body scans for seal PH1802 were evaluated in both inflated and non-inflated conditions to determine changes in respiratory tract volume and total body volume. The increase in respiratory tract volume was 815 mL. In contrast, total body volume in the inflated condition increased by only 446 mL; this was equivalent to a 2% increase in body volume. The directly measured surface area of this seal was 58,193 cm^2 and its total body volume was 25,004 cm^3, resulting in a SA:V of 2.3:1. For the two seals for which total blubber volume could be directly measured from CT scans, blubber by total body volume was 33% (PH1804) and 49% (PH1802).

Allometry

The equation we determined for pinnipeds generated from previously published values ($TLC=0.1M_b^{0.98}$) is remarkably close to the classic relationship reported by Kooyman, 1989 for marine mammals (Figure 2). The Kooyman equation falls within the 95% confidence interval of the pinniped-only equation, indicating that this offset is not significant. The source data for the pinniped-only relationship are provided in Table S2 (Burns et al., 2007; Falke et al., 2008; Kooyman and Sinnett, 1982; Lenfant et al., 1970; Lydersen et al., 1992; Reed et al., 1994). The ringed seals in this study are the smallest pinnipeds for which TLC data are now available. When compared to the scaling relationships described above, our *in vivo* measurements obtained from ringed seals are 26% to 29% lower than predicted.

Body density and net buoyant force

Body density and buoyant force were calculated from the measured total body volume of one individual (PH1804) in the inflated condition, and another individual (PH1802) in both non-inflated and inflated conditions. Taking body mass into account, both seals exhibited similar body density irrespective of inflation condition. Individual PH1802 was denser than seawater (1.027 g mL^{-1} at 10°C) at both 0 mmHg (1.052 g mL^{-1}) and 30 mmHg (1.033 g mL^{-1}) inflation conditions, whereas seal PH1804 was less dense than seawater (0.989 g mL^{-1}) in the inflated condition. Based on these measurements PH1802 had negative calculated buoyant forces in both non-inflated (-6.0 N) and inflated (-1.5 N) conditions. In contrast, PH1804 had a positive buoyant force of 7.6 N in the inflated condition.

Discussion

We used opportunistic biomedical imaging to improve understanding of key respiratory parameters in living ringed seals. These data allowed for re-evaluation of allometric relationships for marine mammal species at the smallest end of the continuum. Further, we leveraged whole body scan data to gain insight into potential challenges faced by a small-bodied species managing dynamic buoyant forces at depth.

Volumetric reconstruction showed that the anatomical dead space of ringed seals comprised only 3% of total respiratory tract volume and changed little between non-inflated and inflated conditions. This negligible change can be attributed to the rigid hyaline cartilage reinforcement of the trachea (Smodlaka et al., 2009), which aids in lung collapse while diving by allowing compressed air from the lungs to be stored within this non-compliant compartment (Kooyman, 1973). The largest capacity of the air-filled respiratory tract—including dead space and lung volume—was 2.3 L. On average, TLC was three times smaller in our ringed seals measured *in vivo* than in ringed seal lungs assessed following death (Lydersen et al., 1992). This could be due in part to the relevant constraints of lung inflation within an enclosed body cavity versus when the respiratory tract is excised. While differences in development may confound comparisons across age classes, mass-specific TLC of our immature seals was also smaller than measures obtained from the excised lungs of adult seals (Lydersen et al., 1992), suggesting that postmortem measurements may overestimate lung volume.

Given hyperinflation of the lungs during prescribed veterinary assessments, our measurements provide an upper bound of TLC. The higher pressures applied were intended to prevent atelectasis. Notably, we found little difference in TLC at pressures of 30- and 37-mmHg, indicating that lungs reached maximum expansion in both conditions. While normally measured at a pressure of 22 mmHg, we believe the TLC values reported here are biologically relevant as they capture full inflation of the lungs within the body cavity. Indeed, patient positioning had a greater influence on TLC than inflation pressure. Within the same individual, TLC was 13% greater in dorsal than in ventral recumbency, highlighting the effect of gravity and body positioning on TLC estimates obtained out of water. It appears that measurements conducted in dorsal recumbency allow for more complete expansion of the lungs and chest wall and facilitate more accurate assessments of TLC.

We measured minimum air volumes that were about 40% of TLC. This is much higher than values based on excised respiratory tracts in other marine mammals, which indicate MAV is 0 to 16% of TLC (Fahlman et al., 2011; Kooyman and Sinnett, 1979). Although it is a common metric, MAV can be difficult to compare across studies. Here, MAV was measured in living, apneic seals when lungs were relaxed in the non-inflated condition. Other studies have defined MAV as the volume of relaxed lungs when transpulmonary pressure is zero (Kooyman and Sinnett, 1979), a condition that can only be achieved postmortem. MAV has also been related to both functional residual capacity (FRC – air volume remaining after a passive exhalation) and residual volume (RV – air volume remaining after forceful exhalation) in living animals (Fahlman et al., 2011). Our definition of MAV most closely aligns with FRC; therefore, comparisons to postmortem studies of other marine mammals may not be appropriate.

Diving lung volumes (DLV) are commonly estimated at 50% of TLC for pinnipeds, with an oxygen extraction efficiency of 15% (Kooyman, 1973; Kooyman and Sinnett, 1982; Kooyman et al., 1971). As direct measurements exist for only a small subset of species (Kooyman et al., 1971; Ponganis, 2011), we often rely on these assumptions to quantify mass-specific DLV. For our ringed seals, the traditional assumptions yield a DLV ranging from 0.4 – 1.1 L and corresponding mass-specific diving lung oxygen stores from 3.9 – 6.9 mL kg^{-1}. Similar to TLC, these values for DLV in immature ringed seals are lower than previously reported for adult ringed seals (Lydersen et al., 1992), and more similar to values reported for harbor seal pups (Burns et al., 2005). Although the assumptions outlined above can be useful in estimating DLV when empirical data are lacking, much remains to be learned about how respiratory capacities including DLV may change across ontogeny.

Relative to predictions based on scaling relationships, the immature ringed seals in this study had lower than expected lung volumes. This was also the case for adult ringed seals measured postmortem (Lydersen et al., 1992), suggesting that the low values obtained here are not explained by methodology or ontogeny. Rather, we propose that the deviation of ringed seal lungs from common scaling relationships is related to their compact body size and extensive blubber stores. One of the novel aspects of this work was our ability to directly measure the SA:V of one individual. This metric is rarely empirically determined but is relevant to several aspects of thermoregulation, hydrodynamics, and energetics. To compensate for large SA:V and associated heat loss in polar waters, ringed seals have considerable blubber reserves that may comprise half their body volume. Although serving different primary functions, both lungs and blubber have important effects on buoyancy, which may explain their relative proportions in the smallest phocid.

Seals must manage dynamic buoyant forces while diving; as such, estimates of net buoyancy are of ecological interest. The imaging approach employed here enabled volumetric measurements relevant to constraints on diving beyond the air-filled respiratory tract. Despite high blubber content (48% of body volume), seal PH1802 had a negative buoyant force in both inflated and non-inflated lung conditions. In contrast, seal PH1804 had lower blubber volume (33% of body volume) but exhibited a positive buoyant force. These surprising results underscore the importance of body composition. Both seals were nearly equivalent to the density of seawater, suggesting that small changes in blubber content and/or lung volume can have meaningful effects on buoyancy and the overall cost of diving. The relatively small lungs of ringed seals may offset the increased positive buoyant force resulting from their extreme blubber reserves. Though not directly examined here, others have demonstrated trade-offs between body condition, dive behavior, and diving energetics (Adachi et al., 2014; Nousek-McGregor et al., 2014; Richard et al., 2014; Watanabe et al., 2006; Webb et al., 1998; Williams et al., 2000) that are likely relevant to wild ringed seals.

We conclude that *in vivo* measurements of lung volume in ringed seals are smaller in both absolute and mass-specific terms relative to postmortem assessments. Further, total body mass consistently underestimates TLC in this species when considered in the context of established allometric relationships. This deviation likely results from their small, compact body size and exceptional blubber stores. Perspectives enabled by biomedical imaging can provide accurate quantification of specific regions of the respiratory tract, as well as additional measures of total body and blubber volume that have important ecological implications for free-ranging individuals.

References

Adachi, T., Maresh, J. L., Robinson, P. W., Peterson, S. H., Costa, D. P., Naito, Y., Watanabe, Y. Y. and Takahashi, A. (2014). The foraging benefits of being fat in a highly migratory marine mammal. *Proc. R. Soc. B Biol. Sci.* **281**, 1–9.

Burns, J. M. and Castellini, M. A. (1996). Physiological and behavioral determinants of the aerobic dive limit in Weddell seal (Leptonychotes weddellii) Pups. *J. Comp. Physiol. B* **166**, 473–483.

Burns, J. M., Costa, D. P., Frost, K. and Harvey, J. T. (2005). Development of Body Oxygen Stores in Harbor Seals: Effects of Age, Mass, and Body Composition. *Physiol. Biochem. Zool.* **78**, 1057–1068.

Burns, J. M., Lestyk, K. C., Folkow, L. P., Hammill, M. O. and Blix, A. S. (2007). Size and distribution of oxygen stores in harp and hooded seals from birth to maturity. *J. Comp. Physiol. B Biochem. Syst. Environ. Physiol.* **177**, 687–700.

Butler, P. J. and Jones, D. R. (1997). Physiology of diving of birds and mammals. *Physiol. Rev.* **77**, 837–99.

Chevalier, P. A., Rodarte, J. R. and Harris, L. D. (1978). Regional lung expansion at total lung capacity in intact vs. excised canine lungs. *J. Appl. Physiol.* **45**, 363–369.

Denison, D. M. and Kooyman, G. L. (1973). The structure and function of the small airways in pinniped and sea otter lungs. *Respir. Physiol.* **17**, 1–10.

Denison, D. M., Warrell, D. A. and West, J. B. (1971). Airway structure and alveolar emptying in the lungs of sea lions and dogs. *Respir. Physiol.* **13**, 253–260.

Fahlman, A., Loring, S. H., Ferrigno, M., Moore, C., Early, G., Niemeyer, M., Lentell, B., Wenzel, F., Joy, R. and Moore, M. J. (2011). Static inflation and deflation pressure-volume curves from excised lungs of marine mammals. *J. Exp. Biol.* **214**, 3822–3828.

Fahlman, A., Loring, S. H., Johnson, S. P., Haulena, M., Trites, A. W., Fravel, V. A. and Van Bonn, W. G. (2014). Inflation and deflation pressure-volume loops in anesthetized pinnipeds confirms compliant chest and lungs. *Front. Physiol.* **5**, 1–7.

Fahlman, A., Sato, K. and Miller, P. (2020). Improving estimates of diving lung volume in air-breathing marine vertebrates.

Falke, K. J., Busch, T., Hoffmann, O., Liggins, G. C., Liggins, J., Mohnhaupt, R., Roberts, J. D., Stanek, K. and Zapol, W. M. (2008). Breathing pattern, CO2 elimination and the absence of exhaled NO in freely diving Weddell seals. *Respir. Physiol. Neurobiol.* **162**, 85–92.

Fedorov, A., Beichel, R., Kalpathy-Cramer, J., Finet, J., Fillion-Robin, J.-C., Pujol, S., Bauer, C., Jennings, D., Fennessy, F. M., Sonka, M., et al. (2012). *3D Slicer as an Image Computing Platform for the Quantitative Imaging Network.*

Fowler, W. S. (1948). Lung Function Studies. II. The Respiratory Dead Space. *Am. J. Physiol. Content* **154**, 405–416.

Goertz, C. E. C., Gray, M. and Tuomi, P. (2008). Long-Term Catheters for Phocids Undergoing Rehabilitation. In *AAZV Annual Conference*, p. Anchorage, Alaska.

Kooyman, G. L. (1973). Respiratory Adaptations in Marine Mammals. *Am. Zool.* **13**, 457–468.

Kooyman, G. L. (1989). *Diverse divers: physiology and behavior*. Berlin Heidelberg New York: Springer-Verlag.

Kooyman, G. L. and Sinnett, E. E. (1979). Mechanical properties of the harbor porpoise lung, Phocoena phocoena. *Respir. Physiol.* **36**, 287–300.

Kooyman, G. L. and Sinnett, E. E. (1982). Pulmonary Shunts in Harbor Seals and Sea Lions during Simulated Dives to Depth. *Physiol. Zool.* **55**, 105–111.

Kooyman, G. L., Kerem, D. H., Campbell, W. B. and Wright, J. J. (1971). Pulmonary function in freely diving Weddell seals, Leptonychotes weddelli. *Respir. Physiol.* **12**, 271–282.

Kooyman, G., Schroeder, J., Denison, D., Hammond, D., Wright, J. and Bergman, W. (1972). Blood nitrogen tensions of seals during simulated deep dives. *Am. J. Physiol. Content* **223**, 1016–1020.

Lenfant, C., Johansen, K. and Torrance, J. D. (1970). Gas transport and oxygen storage capacity in some pinnipeds and the sea otter. *Respir. Physiol.* **9**, 277–286.

Loring, S. H., Topulos, G. P. and Hubmayr, R. D. (2016). Transpulmonary Pressure: The Importance of Precise Definitions and Limiting Assumptions. *Am. J. Respir. Crit. Care Med.* **194**, 1452–1457.

Lydersen, C., Ryg, M. S., Hammill, M. O. and O'Brien, P. J. (1992). Oxygen stores and aerobic dive limit of ringed seals (Phoca hispida). *Can. J. Zool.* **70**, 458–461.

Mitchell, G. and Skinner, J. D. (2011). Lung volumes in giraffes, Giraffa camelopardalis. *Comp. Biochem. Physiol. Part A Mol. Integr. Physiol.* **158**, 72–78.

Mitzner, W., Brown, R. and Lee, W. (2001). In vivo measurement of lung volumes in mice. *Physiol. Genomics* **4**, 215–221.

Moore, M. J., Hammar, T., Arruda, J., Cramer, S., Dennison, S., Montie, E. and Fahlman, A. (2011). Hyperbaric computed tomographic measurement of lung compression in seals and dolphins. *J. Exp. Biol.* **214**, 2390–2397.

Nevitt, B. N., Langan, J. N., Adkesson, M. J., Mitchell, M. A., Henzler, M. and Drees, R. (2014). Comparison of air sac volume, lung volume, and lung densities determined by use of computed tomography in conscious and anesthetized Humboldt penguins (Spheniscus humboldti) positioned in ventral, dorsal, and right lateral recumbency. *Am. J. Vet. Res.* **75**, 739–745.

Noren, S. R., Iverson, S. J. and Boness, D. J. (2005). Development of the blood and muscle oxygen stores in gray seals (Halichoerus grypus): Implications for juvenile diving capacity and the necessity of a terrestrial postweaning fast. *Physiol. Biochem. Zool.* **78**, 482–490.

Nousek-McGregor, A. E., Miller, C. A., Moore, M. J. and Nowacek, D. P. (2014). Effects of Body Condition on Buoyancy in Endangered North Atlantic Right Whales. *Physiol. Biochem. Zool.* **87**, 160–171.

Ponganis, P. J. (2011). Diving Mammals. *Compr. Physiol.* **1**, 447–465.

Ponganis, P. (2015). *Diving Physiology of Marine Mammals and Seabirds*. Cambridge: Cambridge University Press.

Ponganis, P. J. and Williams, C. L. (2016). Oxygen stores and diving. In *Marine Mammal Physiology: Requisites for Ocean Living* (ed. Castellini, M. A.) and Mellish, J.-A.), pp. 29–43. Boca Raton, FL.

Ponganis, P. J., Kooyman, G. L., Sartoris, D. and Jobsis, P. (1992). Pinniped splenic volumes. *Am. J. Physiol. Integr. Comp. Physiol.* **262**, R322–R325.

Ponganis, P. J., St Leger, J. and Scadeng, M. (2015). Penguin lungs and air sacs: implications for baroprotection, oxygen stores and buoyancy. *J. Exp. Biol.* **218**, 720–730.

Reed, J. Z., Chambers, C., Fedak, M. a and Butler, P. J. (1994). Gas exchange of captive freely diving grey seals (Halichoerus grypus). *J. Exp. Biol.* **191**, 1–18.

Richard, G., Vacquie-Garcia, J., Jouma'a, J., Picard, B., Genin, A., Arnould, J. P. Y., Bailleul, F. and Guinet, C. (2014). Variation in body condition during the post-moult foraging trip of southern elephant seals and its consequences on diving behaviour. *J. Exp. Biol.* **217**, 2609–2619.

Rossier, P. H. and Bühlmann, A. (1955). The Respiratory Dead Space. *Physiol. Rev.* **35**, 860–876.

Scholander, P. F. (1940). *Experimental investigations on the respiratory function in diving mammals and birds*.

Smodlaka, H., Henry, R. W. and Reed, R. B. (2009). Macroscopic Anatomy of the Ringed Seal [Pusa (Phoca) hispida] Lower Respiratory System. *Anat. Histol. Embryol.* **38**, 177–183.

Soutiere, S. E. and Mitzner, W. (2004). On defining total lung capacity in the mouse. *J. Appl. Physiol.* **96**, 1658–1664.

Standaert, T. A., LaFramboise, W. A., Tuck, R. E. and Woodrum, D. E. (1985). Serial determination of lung volume in small animals by nitrogen washout. *J. Appl. Physiol.* **59**, 205–10.

Sue, D. Y. (2013). Measurement of Lung Volumes in Patients with Obstructive Lung Disease. A Matter of Time (Constants). *Ann. Am. Thorac. Soc.* **10**, 525–530.

Thometz, N. M., Murray, M. J. and Williams, T. M. (2015). Ontogeny of Oxygen Storage Capacity and Diving Ability in the Southern Sea Otter (Enhydra lutris nereis): Costs and Benefits of Large Lungs. *Physiol. Biochem. Zool.* **88**, 311–27.

Wanger, J., Clausen, J. L., Coates, A., Pedersen, O. F., Brusasco, V., Burgos, F., Casaburi, R., Crapo, R., Enright, P., van der Grinten, C. P. M., et al. (2005). Standardisation of the measurement of lung volumes. *Eur. Respir. J.* **26**, 511–22.

Watanabe, Y., Baranov, E. A., Sato, K., Naito, Y. and Miyazaki, N. (2006). Body density affects stroke patterns in Baikal seals. *J. Exp. Biol.* **209**, 3269–3280.

Webb, P. M., Crocker, D. E., Blackwell, S. B., Costa, D. P. and Le Boeuf, B. J. (1998). Effects of Buoyancy on the Diving Behavior of Northern Elephant Seals. *J. Exp. Biol.* **201**, 2349–58.

Weibel, E. R. (1973). Morphological basis of alveolar-capillary gas exchange. *Physiol. Rev.* **53**, 419–95.

Williams, T. M., Davis, R. W., Fuiman, L. A., Francis, J., Le Boeuf, B. J., Horning, M., Calambokidis, J. and Croll, D. A. (2000). Sink or Swim: Strategies for Cost-Efficient Diving by Marine Mammals. *Science (80-.).* **288**, 133–136.

Woodie, K., Reichmuth, C., Goertz, C., Belovarac, J. and McMillen, S. (2020). Clinical Sedation of Alaskan Phocid Seals. In *Alaska Marine Science Symposium*, p. Anchorage, Alaska.

Tables & Figures

Table 1. Respiratory volume parameters for individual ringed seals in non-inflated and inflated conditions, shown with measures of body volume and corresponding body density and buoyancy. Diving lung volume is estimated as 50% of TLC. Usable lung oxygen is calculated based on 15% oxygen extraction efficiency.

Individual	PH1701[a]	PH1503[a]	PH1804[b]	PH1802[c]	
Sex	F	M	M	M	
Age (months)	15.6	43	16.7	25.8	
Mass (kg)	14.9	27.5	20.5	26.2	
ST length (cm)	-	90	81.5	86	
Non-inflated (0 mmHg)					**Range**
Trachea volume (mL)	-	39.9	-	26.2	26.2 - 39.9
Trachea volume (mL kg^{-1})	-	1.4	-	1.0	1.0 - 1.4
Bronchi volume (mL)	-	9.9	-	9.3	9.3 - 9.9
Bronchi volume (mL kg^{-1})	-	0.4	-	0.4	0.4
L lung volume (mL)	-	465	-	262	262 - 465
R lung volume (mL)	-	421	-	302	302 - 421
Total lung volume (mL)	-	886	-	564	564 - 886
Total lung volume (mL kg^{-1})	-	32.2	-	21.5	21.5 - 32.2
Total respiratory tract volume (mL)	-	936	-	599	599 - 936
Total body volume (mL)	-	-	-	24913	-
Body density (g mL^{-1})	-	-	-	1.052	-
Buoyant force (N)	-	-	-	-6.0	-

Inflated (30 mmHg)					
Trachea volume (mL)	23.1	43.1	34.6	32.2	23.1 - 43.1
Trachea volume (mL kg^{-1})	1.6	1.6	1.7	1.2	1.2 - 1.7
Bronchi volume (mL)	11.2	9.1	13.7	10.3	9.1 - 13.7
Bronchi volume (mL kg^{-1})	0.8	0.3	0.7	0.4	0.3 - 0.8
L lung volume (mL)	426	1108	912	650	426 - 912
R lung volume (mL)	444	1163	977	723	444 - 1163
Total lung volume (mL)	870	2271	1890	1372	870 - 2271
Total lung volume (mL kg^{-1})	58.4	82.6	92.2	52.4	52.4 - 92.2
Diving lung volume (L)	0.4	1.1	0.9	0.7	0.4 – 1.1
Usable lung O_2 (L)	0.1	0.2	0.1	0.1	0.1 – 0.2
Diving lung O_2 store (mL kg^{-1})	4.4	6.2	6.9	3.9	3.9 – 6.9
Total respiratory tract volume (mL)	904	2323	1938	1415	904 - 2323
Total body volume (mL)	-	-	20719	25359	20719 - 25359
Body density (g mL^{-1})	-	-	0.989	1.033	0.989 - 1.033
Buoyant force (N)	-	-	7.6	-1.5	-1.5 – 7.6
Difference respiratory tract %	-	148%	-	136%	-
Difference total body volume %	-	-	-	2%	-
Difference total body volume (mL)				446.6	

CT Scanner Model: [a] GE 16 Slice Light Speed, [b] GE 16 Slice Bright Speed, [c] Siemens 32/64 Somatom GO-UP

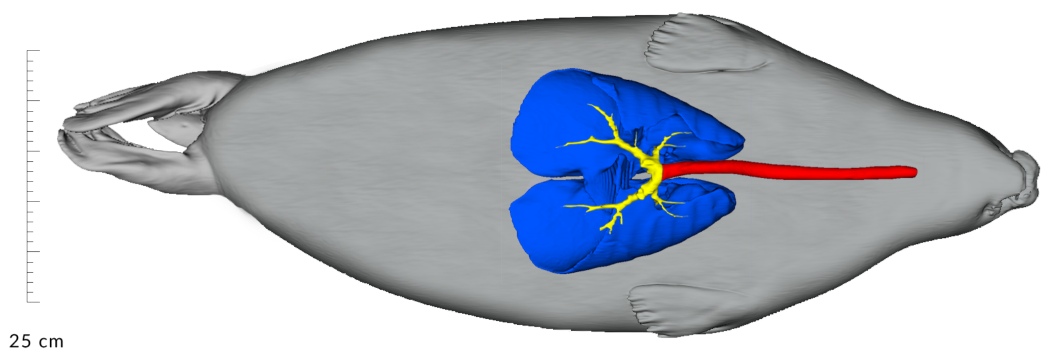

Figure 1. 3D reconstruction of ringed seal PH1802 at lung inflation pressure of 30 mm Hg. Ventral side of animal shown with body contour in grey. The trachea is red, bronchi are yellow, and lungs are blue. See S1 for video of 3D reconstruction in both non-inflated and inflated conditions. (color online)

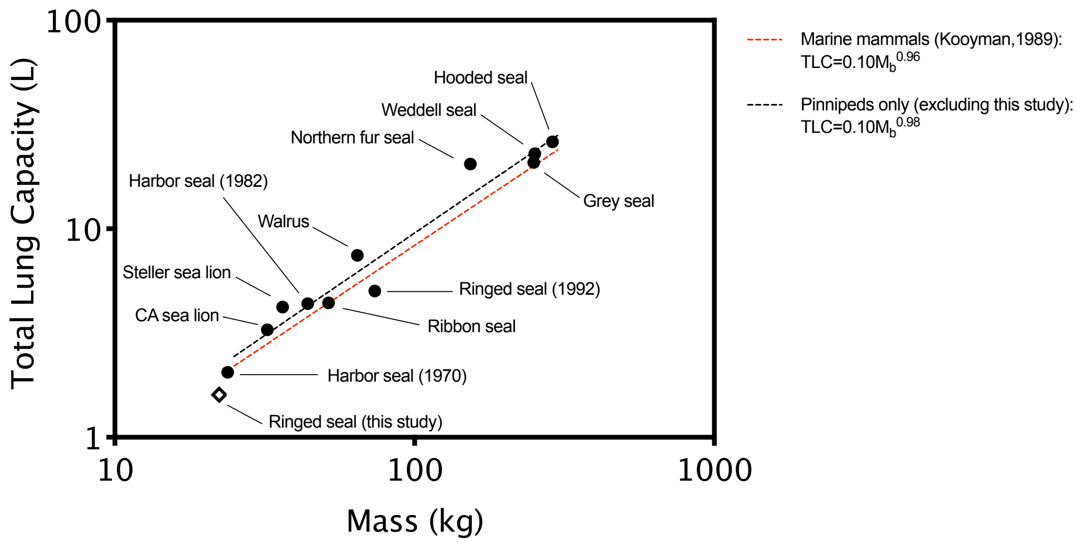

Figure 2. Logarithmic plot of mean total lung capacity (TLC, liters) as a function of body mass (kg). Kooyman's (1989) allometric scaling equation for marine mammals, TLC=0.1M$_b^{0.96}$ (red dashed line) is plotted with pinniped-only relationship determined in this study, TLC=0. 1M$_b^{0.98}$ (black dashed line). Kooyman's (1989) allometric relationship falls within the bounds of the 95% confidence interval of the pinniped-only allometric line, indicating that the two equations are not significantly different. Source data for pinniped-only line are provided in Table S2. Ringed seals from this study are shown as a group mean (n=4).

Appendices

Table S 1. Modified chest CT imaging protocols for ringed seal cases shown in Table 1.

	GE 16 Slice Light Speed	GE 16 Slice Bright Speed	Siemens 32/64 Somatom GO-UP
Scan type	Helical full	Helical full	Helical full
Rotation time (s)	0.5	0.5	1.5, 1.0 (opt 0.8)
Beam collimation (mm)	20	20	-
Thickness (mm)	0.6250 – 2.50	0.6250 – 2.50	2.0
Spiral pitch factor	1.35	1.35	0.8
Speed (mm/rotation)	27.5	27.5	17.89
Reconstruction interval	5	5	2.0
Gantry tilt	0	0	0
Gantry period	-	0.60	-
Scan FOV	Large	Large	Whole body
kVp	120	120	130
Xray tube current (mA)	100 – 440	100 – 440	28
Noise index	11.57	11.57	15
Dose reduction	260	260	On - 3
Algorithm	Standard	Standard	Standard
Reformats	Full	Full	Full

Table S 2. Lung oxygen stores for marine carnivores, showing the ringed seals in this study with comparative values for other species. Species for which total lung capacity (TLC) is available are plotted in Figure 2. Diving lung volume (DLV) O_2 store calculated based on assumption that DLV is 50% of TLC for pinnipeds. Usable O_2 for gas exchange is estimated as 15% of DLV (Kooyman, 1989), and reported as mass-specific diving lung volume oxygen store (DLV O_2 store). Data are provided for individuals when possible (n=1), or as grouped mean values (n>1).

Species	Age	Mass (kg)	Sample (n)	TLC (L)	DLV (L)	DLV O_2 store (mL kg^{-1})	Method	Reference
Phocids								
Ringed seal *Pusa hispida*	subadult	26.2	1	1.37	0.69[††]	3.9[j]	in vivo[f]	A
		20.5	1	1.89	0.94[††]	6.9[j]	in vivo[f]	A
		27.5	1	2.27	1.14[††]	6.2[j]	in vivo[f]	A
		14.9	1	0.87	0.44[††]	4.4[j]	in vivo[f]	A
	adult	73.7[†]	50	5.04 ± 1.24[†]	2.52[††]	6.8[j]	postmortem[a]	B
Harbor seal *Phoca vitulina*	mixed	23.8[†]	5	2.05[†]	1.03[††]	6.5[j]	postmortem[a]	C
	neonatal	10.3 ± 0.4[†]				5.3[k]	postmortem[a]	D
	nursing pup	24.9 ± 1.5[†]				5.3[k]	postmortem[a]	D
	weaned pup	28.9 ± 0.5[†]	395			5.3[k]	postmortem[a]	D
	yearling	33.1 ± 0.5[†]				-	postmortem[a]	D
	adult	52.1 ± 1.6[†]				12.2[k]	postmortem[a]	D
	subadult	44	1	4.4			in vivo[c]	L
	subadult	40	1	4			in vivo[c]	L
	subadult	36	1	3.6			in vivo[c]	L
	subadult	52	1	5.1			in vivo[c]	L
	subadult	48	1	4.8			in vivo[c]	L
Grey seal *Halichoerus grypus*	pup	40.1 ± 1.3	10			4.1[k]	in vivo[c]	E
	yearling	51.6 ± 2.7[†]	10			4.1[k]	in vivo[c]	E
	adult female	191.5 ± 6.0[†]	10			4.1[k]	in vivo[c]	E

	adult	250[†]	4	20.81[†]	10.4[††]	6.2[j]	in vivo[c]	F
Ribbon seal *Histriophoca fasciata*	adult	51.7[†]	4	4.42[†]	2.2[††]	6.4[j]	postmortem[a]	C
Harp seal *Pagophilus groenlandicus*	neonatal	10.3 ± 1.1[†]					postmortem[e]	G
	nursing pup	29.4 ± 1.1[†]					postmortem[e]	G
	weaned pup	36.6 ± 1.1[†]	40				postmortem[e]	G
	yearling	29.3 ± 1.6[†]					postmortem[e]	G
	adult	115.4 ± 4.7[†]					postmortem[e]	G
Hooded seal *Cistophora cristata*	adult female	252.1 ± 17.9[†]	6	(22.9)		6.8[k]	postmortem[e]	G
	nursing pup	38.5 ± 12.5[†]	2	(1.4)		2.8[k]	postmortem[e]	G
	weaned pup	48.1 ± 2[†]	6	(2.0)		3.1[k]	postmortem[e]	G
Weddell seal *Leptonychotes weddellii*	pup	106	1			4.1[†, k]	in vivo[c]	H
		137	1			4.1[†, k]	in vivo[c]	H
		124	1			4.1[†, k]	in vivo[c]	H
		107	1			4.1[†, k]	in vivo[c]	H
	subadult	260	1	(22.2)	11.1	6.4[j]	*in vivo*[b, h]	I
		345	1	(23.6)	11.8	5.1[j]	*in vivo*[b, h]	I
		261	1	(32.6)	16.3	9.4[j]	*in vivo*[b, h]	I
	adult	425[†]	4		14	4.1[†, j]	*in vivo*[b]	J
					14	4.1[†, j]	*in vivo*[b]	J
				Scruffy	11	4.1[†, j]	*in vivo*[b]	J
					20	4.1[†, j]	*in vivo*[b]	J
					7	4.1[†, j]	*in vivo*[b]	J
					20	4.1[†, j]	*in vivo*[b]	J

				Gentle Ben	13	4.1[†, j]	*in vivo* [b]	J
					7	4.1[†, j]	*in vivo* [b]	J
					13	4.1[†, j]	*in vivo* [b]	J
				Ringo	8	4.1[†, j]	*in vivo* [b]	J
					5	4.1[†, j]	*in vivo* [b]	J
					13	4.1[†, j]	*in vivo* [b]	J
					6	4.1[†, j]	*in vivo* [b]	J
Otariids								
Northern fur seal *Callorhinus ursinus*	mixed	153.5[†]	4	20.45[†]	10.2[††]	10.0 [j]	postmortem [a]	C
Steller sea lion *Eumetopias jubatus*	mixed	36.3[†]	4	4.22[†]	2.1[††]	8.7 [j]	postmortem [a]	C
	neonatal	22[†]	1	1.96[†]	1.0[††]	6.7 [j]	postmortem [a]	C
Odobenids								
Walrus *Odobenus rosmarus*	mixed	64.5[†]	3	7.45[†]	3.7[††]	8.7 [j]	postmortem [a]	C
Mustelids								
Northern sea otter *Enhydra lutris lutris*	adult	27.6[†]	3	9[†]	5.7	31.0 [j]	postmortem [a]	C
Southern sea otter *Enhydra lutris nereis*	neonatal	2.6 ± 0.18[†]	5			42.7 ± 3.09 [k]	postmortem[i]	K
	small pup	4.4 ± 0.30[†]	2			48.7 ± 7.31 [k]	postmortem[i]	K
	large pup	8.5 ± 0.62[†]	4			41.6 ± 4.56 [k]	postmortem[i]	K
	juvenile	12.2 ± 0.99[†]	3			41.6 ± 1.60 [k]	postmortem[i]	K
	adult	19.9 ± 1.01[†]	6			31.1 ± 2.30 [k]	postmortem[i]	K

References: A: this study; B: Lydersen et al., 1992; C: Lenfant et al., 1970; D: Burns et al., 2005; E: Noren et al., 2005; F: Reed et al., 1994; G: Burns et al., 2007; H: Burns and Castellini, 1996; I: Falke et al., 2008; J: Kooyman et al., 1971; K: Thometz et al., 2015; L: Kooyman and Sinnett, 1982. Values represented within parentheses were back-calculated from diving lung volumes.

[a] Inflation of excised lungs via water displacement; [b] Nitrogen washout; [c] Author calculated or used values based on allometric equations established in other studies; [d] Author calculated based on allometric equations established from study itself; [e] Used combination of inflation of excised lungs and calculations from allometric equations established from study itself; [f] *In vivo* biomedical imaging; [g] Whole body plethysmography; [h] Pneumotachograph; [i] Used body size, lung mass, and empirical measures of lung volume to calculate TLC and DLV; [j] Value calculated here from usable O_2 and body mass. Mass-specific DLV O_2 store from southern sea otters used to calculate mass-specific DLV O_2 store for northern sea otters; [k] Value reported in original publication referenced; [†] Published value was either a mean with no individual value available or was given as a range with only one value for TLC calculated; in these cases, sample size is given; [††] Value calculated here based on assumption that DLV for pinnipeds is 50% of TLC, with 15% of DLV being usable O_2 for oxygen exchange (Kooyman, 1989). Usable O_2 (liters) for northern sea otters calculated from mass-specific DLV of southern sea otter adults measured in Thometz et al., 2015